Published in final edited form as:

Structure. 2017 March 07; 25(3): 496–505. doi:10.1016/j.str.2017.02.001.

Human βB2-crystallin forms a face-en-face dimer in solution - an integrated NMR and SAXS study

Zhaoyong Xi[1], **Matthew J. Whitley**[1], and **Angela M. Gronenborn**[1,2,*]

[1]Department of Structural Biology, University of Pittsburgh School of Medicine, Pittsburgh, PA, 15261, USA

Summary

βγ-crystallins are long-lived eye lens proteins that are crucial for lens transparency and refractive power. Each βγ-crystallin comprises two homologous domains, which are connected by a short linker. γ-crystallins are monomeric, while β-crystallins crystallize as dimers and multimers. In the crystal, human βB2-crystallin is a domain-swapped dimer, while the N-terminally truncated βB1-crystallin forms a face-en-face dimer. Combining and integrating data from multi-angle light scattering, NMR and small angle X-ray scattering of full-length and terminally truncated human βB2-crystallin in solution, we show that both these βB2-crystallin proteins are dimeric, possess C2 symmetry, and are more compact than domain-swapped dimers. Importantly, no intermolecular paramagnetic relaxation enhancement effects compatible with domain-swapping were detected. Our collective experimental results unambiguously demonstrate that, in solution, human βB2-crystallin is not domain-swapped and exhibits a face-en-face dimer structure similar to the crystal structure of truncated βB1-crystallin.

Graphical abstract

*Correspondence: amg100@pitt.edu.
[2]Lead Contact

Author Contributions

A.M.G. supervised the overall project. Z.X. and A.M.G. designed the research. Z.X. performed the MALS and NMR experiments. Z.X. and M.J.W. performed the SAXS experiments. Z.X. and A.M.G. analyzed the data and wrote the manuscript. All authors discussed the results, commented and approved the manuscript.

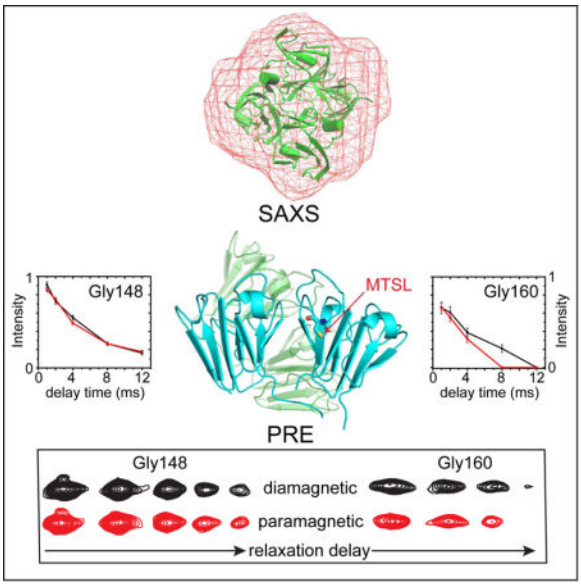

Keywords

NMR; SAXS; PRE; βB2-crystallin; domain-swapping

Introduction

Crystallins, the predominant structural proteins in the eye lens, play an essential role in maintaining lens transparency and refractive index (Andley, 2007; Bloemendal et al., 2004). The proteins belong to two different superfamilies, named α- and βγ-crystallins. In the eye lens, α-crystallins assemble into high-order oligomers and function as molecular chaperones to protect the eye lens against physiological stress (Bloemendal et al., 2004; Haslbeck et al., 2016). βγ-crystallins, which account for around 50% of the protein mass in the human lens, are considered to be the refractive proteins, responsible for maintaining lens transparency (Andley, 2007; Bloemendal et al., 2004). Short-range interactions between βγ-crystallins are believed to provide a uniform concentration gradient that contributes to lens refraction and transparency (Andley, 2007; Takemoto and Sorensen, 2008). While γ-crystallins are monomeric, β-crystallins associate into various homo- and hetero-oligomers (Bloemendal et al., 2004; Slingsby and Wistow, 2014).

All lens βγ-crystallins possess two similar domains, connected by a short inter-domain linker. Each domain comprises two Greek key motifs packed into a β-sheet sandwich (Figure 1). Human β- and γ-crystallins share highly homologous sequences, with all β-crystallins containing terminal extensions, which may be a factor in their dimer or high-order oligomer formation (Bloemendal et al., 2004). β-crystallins can be further classified into two groups, the basic crystallins (βB1, βB2 and βB3) exhibiting both N-terminal and C-terminal extensions and the acidic crystallins (βA1, βA2, βA3 and βA4), which possess only N-terminal extension. βB2-crystallin is generally the predominant β-crystallin in the human eye lens (Robinson et al., 2006). It is also the least modified and most soluble β-crystallin

(Feng et al., 2000; Zhang et al., 2001; Zhang et al., 2003). Furthermore, βB2-crystallin can form hetero-dimers and oligomers with other β-crystallins (Ajaz et al., 1997; Slingsby and Wistow, 2014). It has been reported that βB2-enriched β-crystallin oligomers maintain higher solubility compared to βB2-crystallin devoid oligomeric mixtures (Bateman and Slingsby, 1992; Feng et al., 2000). Co-expression of βB2-crystallin with βA4-crystallin in HeLa cells resulted in abundant soluble βA4-βB2-crystallin hetero-oligomers, whereas βA4-crystallin alone was found to be quickly degraded after expression, even in the presence of αB-crystallin (Marin-Vinader et al., 2006). Thus, it may well be possible that βB2-crystallin may form refractive oligomers with other β-crystallins, thereby acting as a dedicated chaperone for other β-crystallins, thus playing a unique role in maintaining lens transparency.

In the monomeric γ-crystallins the N-terminal (NTD) and C-terminal (CTD) domains are arranged in a pseudo symmetric manner (Figure 1A) (Bloemendal et al., 2004; Slingsby and Wistow, 2014). This kind of intra-molecular domain interaction with a bent linker peptide is also recapitulated in crystal structures of the β-crystallins, except βB2-crystallin. In the crystal structure of human βB2-crystallin, dimerization involves domain swapping between the NTD and CTD, with the inter-domain linker peptide in an extended conformation (Figure 1B) (Smith et al., 2007). This results in a similar domain pairing as in γ-crystallins, albeit with inter-molecular domain interactions. In the crystal lattice, the protein is organized as a dimer of dimers (Figure 1D). The truncated human βB1-crystallin, which exhibits 58% sequence identity to human βB2-crystallin cross domains, also forms a dimer in the crystal structure (Van Montfort et al., 2003). However, in this case, the paired domain interactions are intra-molecular with a bent linker peptide conformation like in γ-crystallins (Figure 1C). Intriguingly, the structure of the truncated βB1-crystallin dimer closely resembles half of the lattice tetramer of βB2-crystallin (Figure 1D). Crystal structures of human βB3- (PDB code 3QK3) and βA4- (PDB code 3LWK) crystallins are also available. βB3-crystallin is a trimer and βA4-crystallin is a dimer, and neither exhibits domain-swapping.

Here, we investigated human βB2-crystallin in solution, using NMR and small angle X-ray scattering (SAXS). Our studies were aimed at elucidating the determinants for domain-swapping in βB2-crystallin. Previous investigations addressed some of the possible causes: (i) The identity of the linker peptide might have been responsible for domain swapping. However, exchanging the linker peptides between γB- and βB2-crystallins did not change the quaternary state of the respective proteins; βB2-crystallin remained dimeric and γB-crystallin a monomer (Mayr et al., 1994; Trinkl et al., 1994). Therefore, domain swapping did not seem to be dependent on the particular amino acid sequence of the linker peptide. (ii) The presence of extensions might have been responsible for domain swapping, since β-crystallins, unlike γ-crystallins, have terminal extensions of different lengths. However, both the N-terminal and C-terminal extensions of βB2-crystallin were observed to be flexible by NMR and are not visible in crystal structures (Bax et al., 1990; Carver et al., 1993; Cooper et al., 1993; Smith et al., 2007). The absence of either or both extensions did not affect the quaternary state of βB2-crystallin (Kroone et al., 1994; Trinkl et al., 1994). (iii) Changing amino acids at the dimer interfaces also did not reverse the domain swapping (Smith et al., 2007). Therefore, no obvious conclusions emerged from these previous studies.

Most domain-swapped protein structures are observed crystallographically and for some proteins it has been established that specific crystallization conditions or other circumstances can cause domain-swapping (Koharudin et al., 2013; Liu et al., 2012; Liu and Eisenberg, 2002). For βB2-crystallin, no solution structural data is available, and no clear picture exists as to the causes for the domain-swapped crystal structures. Here, we applied a combination of solution scattering experiments, multi-angle light scattering (MALS) and small angle X-ray scattering (SAXS), with NMR to investigate the solution structures of full-length and truncated human βB2-crystallin. The MALS and SAXS data revealed that the protein is dimeric and more compact than the crystallographic domain-swapped dimer, respectively, with the SAXS envelope fitting well to one-half of the βB2-crystallin lattice tetramer. In addition, paramagnetic relaxation enhancement (PRE) measurements clearly exclude a domain-swapping arrangement and suggest a face-en-face dimer. Overall, our combined data demonstrate that in solution, human βB2-crystallin adopts a dimeric assembly, similar to the dimer crystal structure of truncated βB1-crystallin, without any evidence for domain swapping.

Results

βB2-crystallin is dimeric and monodisperse in solution

In order to evaluate whether human βB2-crystallin was monomeric or dimeric in solution, MALS measurements were carried out over a broad concentration range (Figure 2). The protein eluted at the same position for all concentrations examined, demonstrating that no higher order association occurs. The experimentally MALS-determined molecular mass (48.8 kDa) is in excellent agreement with the theoretical molecular mass of a dimer (46.5 kDa). The light scattering results unequivocally prove that βB2-crystallin is dimeric in solution, independent of the protein concentration, consistent with previous studies (Bateman et al., 2001; Smith et al., 2007).

To gain insight into the overall solution structure of βB2-crystallin, we performed extensive SAXS analyses on human βB2-crystallin protein solutions at different concentrations. The molecular masses determined based on volumes show that the protein is dimeric in solution (Table S1), in agreement with the MALS data. As evidenced by the data presented in Figure 3, the Guinier plots are linear (Figure 3B), establishing that no aggregation or inter-particle interference is present. The radii of gyration (R_g), calculated from both Guinier approximation and computation of distance distribution function $P(r)$, for the different concentrations are identical within the precision of the measurement (22.7±0.25 Å and 22.6±0.22 Å, respectively; Table S1). Thus, no concentration dependence for R_g or the normalized zero-angle scattering intensity $I(0)$ was observed (Figure S1 and Table S1), further confirming the results from the MALS data that βB2-crystallin is monodisperse in solution. The $P(r)$ analyses show that the maximum diameter, D_{max}, across the protein molecule is independent of concentration, measuring 81.8±1.2 Å (Figure 3C and Table S1). Furthermore, the Kratky plots are bell-shaped curves, asymptotically converging at high q, indicative of a well-folded protein (Figure 3D). Taken together, all of our solution scattering measurements established that βB2-crystallin is dimeric in solution.

SAXS-based structural modeling of full-length βB2-crystallin

Having ascertained that in solution human βB2-crystallin was dimeric, we had to establish which kind of dimer arrangement was present, the domain-swapped arrangement observed in the crystal structure or a different one. This seemed particularly prudent since truncated human βB1-crystallin does not exhibit a domain-swapped dimer in the crystal (Van Montfort et al., 2003). Interestingly, one-half of the crystallographic tetramer of full-length, domain-swapped dimeric βB2-crystallin, enclosed in the red rectangle in Figure 1D, resembles the face-en-face dimer arrangement observed in the crystal of the truncated βB1-crystallin protein (Figure 1C) (Smith et al., 2007). It therefore seemed possible that, in solution, full-length human βB2-crystallin may also form a similar dimer. Thus, both the structure of the domain-swapped dimer and one-half of the lattice tetramer of βB2-crystallin were considered in our analyses.

From the experimental SAXS data, the three-dimensional shape of human βB2-crystallin in solution was constructed using the ATSAS software package (Petoukhov et al., 2012). A low-resolution molecular envelope was created by averaging ten individual *ab initio* bead models (Figure 4A and 4B). The fit between the calculated scattering pattern and the experimental scattering curve is excellent (χ^2 = 0.1435), again demonstrating the high quality of the data. The final SAXS envelope adopts a non-spherical shape, possessing a stalk-like protrusion at one side of the globular object. When superimposed onto the domain-swapped dimer crystal structure, very poor agreement is noted (Figure 4A), while the globular region of the envelope fits significantly better to the coordinates of the pseudo face-en-face dimer extracted from the crystallographic tetramer of human βB2-crystallin (Figure 4B). We also performed CRYSOL comparisons of the theoretical scattering profiles generated from the crystal structures with our experimental SAXS data (Figure 4C and 4D). As can be noted, the overall fit of the domain-swapped dimer structure to the experimental data is poor. The calculated R_g (28.50 Å) from the crystal structure is much larger than the experimental value (22.53 Å), suggesting that a more compact structure is present in solution. By contrast, the comparison with the structure of a face-en-face dimer exhibits a good fit between the theoretical and experimental profiles, with a χ^2 value of 0.355. Therefore, the SAXS data imply that human βB2-crystallin assembles into face-en-face homo-dimers in solution. However, the fit is not perfect and the pseudo dimer structure extracted from the crystallographic tetramer cannot explain the protrusion in the experimental SAXS envelope. We hypothesized that this feature is associated with the existence of the terminal tails, which are present in the protein construct and will contribute to the scattering in solution, whereas they are not in the coordinates of the crystal structure, since no density for the first 13 or last 10 residues was observed (Smith et al., 2007).

In order to test this assumption, we created a shorter construct without the N- and C-terminal extension sequences, comprising exactly the equivalent residues that are visible in the crystal structure of βB2-crystallin, and used this protein for SAXS analysis.

Analysis of the N- and C-terminal truncated βB2-crystallin

We performed MALS characterization of the truncated human βB2-crystallin (14–194), which eluted in a single peak, confirming its quaternary state as dimeric, with an

experimental molecular mass of 41.9 kDa, in excellent agreement with the predicted dimer molecular mass of 41.8 kDa (Figure S2, inset). In addition, careful comparison between the ^{1}H-^{15}N HSQC spectra of truncated and full-length βB2-crystallin showed that the truncation did not result in any significant perturbations of the structure (Figure S2). Only the resonances for the N- and C-terminal residues are missing from the spectrum of the truncated protein and the chemical shifts are essentially identical for the remainder of the residues in both proteins. This is in agreement with previous reports on βB2-crystallins, which showed that the terminal extensions exhibit a large degree of conformational flexibility and that their absence does not affect the dimerization (Carver et al., 1993; Cooper et al., 1993; Kroone et al., 1994; Trinkl et al., 1994).

The shape of the truncated human βB2-crystallin was evaluated by SAXS, as described for the full-length protein above. The truncated protein is monodisperse and well-folded, as evidenced by volume-based molecular mass, the linear Guinier plot, the agreement between the R_g values derived from both Guinier and $P(r)$ analyses, and the Kratky plot (Figure S3 and Table S2). As expected, the truncated protein possesses a lower R_g value than the full-length protein, corresponding to its smaller overall size. Furthermore, the lower D_{max} value (67.0 Å) determined by $P(r)$ analysis clearly indicates that the truncated protein adopts a less anisotropic shape than full-length βB2-crystallin. This conformational change gratifyingly also results in a lack of the protrusion in the SAXS-derived molecular envelope of truncated βB2-crystallin (Figure 4E and 4F), demonstrating that the terminal extensions are responsible for the protrusion in the SAXS envelope of the full-length protein. In addition, superposition of the SAXS envelope onto the structure of the domain-swapped dimer and face-en-face dimer, unequivocally shows a bad fit for the former and an excellent fit to the latter (Figure 4E and 4F). Similarly, the calculated scattering profiles using CRYSOL exhibit good agreement with the experimental profiles for the face-en-face dimer (Figure 4G and 4H). Therefore, taken together, the SAXS data and analyses for both full-length and truncated human βB2-crystallin strongly suggest that the protein is not domain-swapped in solution, but assembles into a face-en-face dimer.

Backbone assignments of wild-type βB2 crystallin and generation of the mutant for spin labeling

NMR has been used for protein structure determination for several decades, and a variety of NMR approaches are available for analyzing protein-protein interactions (Clore and Gronenborn, 1989, 1991; O'Connell et al., 2009; Qin et al., 2001). Here, we used paramagnetic relaxation enhancements (PREs) to determine inter-domain and inter-molecular contacts in the solution dimer of the full-length βB2-crystallin. As a prerequisite, we fully assigned the backbone resonances for full-length βB2-crystallin, using traditional triple resonance experiments. Uniformly deuterated protein was used for improved resolution and sensitivity. In addition, amino acid selective unlabeling was used to verify and confirm the assignments. The final completeness of assignments was ~85%, and the 800 MHz ^{1}H-^{15}N TROSY-HSQC spectrum, recorded on a 350 μM sample at 308 K is shown in Figure 5.

As paramagnetic probe we used the nitroxide spin label MTSL, which is commonly attached to the sulfhydryl group of cysteines. Two conserved cysteines (Cys37 and Cys66) are present in the sequence of human βB2-crystallin. Attachment of the MTSL group to Cys37 caused protein aggregation, although in the structure both cysteines are solvent exposed. We therefore created a C37V mutant and introduced the spin label at Cys66. The structural integrity of the mutant as well as that of the MTSL labeled protein was assessed by ^{1}H-^{15}N HSQC spectroscopy. The C37V mutant exhibited the same dimerization behavior as the wild-type protein and the introduction of spin label did not significantly change the overall conformation of the protein, as evidenced by the excellent superpositions of the ^{1}H-^{15}N HSQC spectra of wild-type, mutant and dMTSL labeled protein (Figure S4). Only very small chemical shift differences were observed for resonances of residues close to the mutation or labeling site.

PREs and domain-domain contacts

PRE measurements were carried out on a number of different MTSL-modified proteins. The first sample contained ^{15}N-C37V mutant protein. As expected, amide groups that are positioned close to the MTSL label experienced the strongest PRE effect, with the corresponding resonances broadened beyond detection in the ^{1}H-^{15}N HSQC spectrum (Figure 6). Since MTSL is located on Cys66, PRE effects for residues in the NTD are expected (Figure 6A). However, some sizable PRE effects were also noted for amides belonging to the CTD (Figure 6B). The presence of inter-domain PREs for this uniformly labeled sample is compatible with either a domain-swapped or the face-en-face dimer. If the dimer is domain-swapped, the extended linker keeps the two domains of the same polypeptide chain apart, and the spin label will not affect the residues in the CTD of the same chain, but in the other chain. By contrast, in a face-en-face dimer, amides of residues in CTD of the same chain will be affected by the spin label. Therefore, in a dimeric sample that is made from the same protein (i.e. identical chains), it is essentially impossible to distinguish the two possible dimeric arrangements, since inter- or intra-chain PRE effects will be measured for the domain-swapped dimer and face-en-face dimer, respectively, as illustrated by the PRE structural mapping in Figure 6C and 6D.

In order to distinguish between inter- and intra-molecular PRE effects, a 1:1 mixed sample of diamagnetically tagged, ^{15}N labeled protein (dMTSL-^{15}N-C37V) and paramagnetically tagged, natural abundance protein (MTSL-^{14}N-C37V) was prepared. Theoretically, this sample will contain 50% mixed dimer (dMTSL-^{15}N-C37V/MTSL-^{14}N-C37V), 25% dMTSL-^{15}N-C37V dimer and 25% MTSL-^{14}N-C37V dimer. If this holds, only the mixed dimer will exhibit PRE effects in the ^{1}H-^{15}N HSQC spectrum, given that the paramagnetic tag resides on an ^{14}N chain, which is not observable in ^{1}H-^{15}N HSQC spectrum. Both other species should be silent, i.e., devoid of PRE effects, since a homo-dimer of MTSL-^{14}N-C37V will not yield a ^{1}H-^{15}N HSQC spectrum and a homo-dimer of dMTSL-^{15}N-C37V does not possess the paramagnetic tag. We used this sample for carefully measuring PREs by recording ^{1}H-^{15}N HSQC spectra for different T_2 relaxation delays. A diamagnetic 1:1 mixed sample of dMTSL-^{15}N-C37V:dMTSL-^{14}N-C37V was used for the control experiments carried out in parallel. A schematic illustration of the possible dimeric arrangements for both para- and dia-magnetic mixed dimers are illustrated in Figure S5. We

then selected resonances that would exhibit PREs if a domain-swapped dimer were present. For the domain-swapped mixed dimer, the MTSL label will affect the amides of some CTD residues in the different chain labeled with ^{15}N (Figure S5B). These residues should also experience the same PRE effects in the uniformly ^{15}N and MTSL labeled sample. We investigated those resonances for which moderate-to-strong PRE effects ($I_{para}/I_{dia}<0.7$, see Figure 5B) were observed in the uniformly labeled sample, and the normalized resonance intensity decays for chosen domain-swap reporter resonances are provided in Figure 7A and Figure S6. Due to the PRE, the intensities of these resonances in the paramagnetic sample are expected to decrease faster as the relaxation delay increases. However, as can be easily appreciated, none exhibited differential intensity decays, and the I_{para}/I_{dia} values for all different relaxation delays were ~1. We further analyzed the PRE data and for a few resonances, such as the amides of residues His132 and Gly160, the intensities decreased faster in the paramagnetic state and disappeared for long relaxation delays (Figure 7B). This observation matches expected contacts for a face-en-face dimer structure. Therefore, our combined PRE data do not support a domain-swapped βB2-crystallin dimer structure in solution, but suggest that a face-en-face dimer, consistent with the SAXS data, has to be present.

Discussion

βγ-crystallins are two-domain proteins that share highly conserved domain structures. Unlike the monomeric γ-crystallins, human β-crystallins can assemble into a wide range of homo- and hetero-oligomers of different sizes (Ajaz et al., 1997). In contrast to other βγ-crystallins, in the crystal structures of human βB2-crystallin variants, different inter-molecular domain interactions are observed (Smith et al., 2007). It may even be possible that different members of the β-crystallin family exchange subunits and an interchange between solvent exposed and buried surfaces may have implications for their extreme solubility and lack of aggregation. Since general determinants for domain-swapping in proteins are still being uncovered, with several cases known where the solution structure does not exhibit domain swapping (Bewley et al., 1998; Gronenborn, 2009; Koharudin et al., 2013; Overduin et al., 1995; Shapiro et al., 1995), we investigated the solution state of full-length βB2-crystallin, the only βγ-crystallin for which a domain-swapped structure has been reported by crystallography (Smith et al., 2007). Integrating results obtained using MALS, SAXS and NMR spectroscopy, we demonstrate that full-length human βB2-crystallin in solution does not exhibit a domain-swapped dimer structure.

Intriguingly, a truncated βB1-crystallin did not crystallize as a domain-swapped dimer, but exhibited a face-en-face dimer (Van Montfort et al., 2003). As the different dimers exhibit distinct overall shapes (Figure 1B and 1C), these two different kinds of dimers should have distinctly different low-resolution SAXS envelope shapes. We found that the experimentally determined SAXS envelope of full-length human βB2-crystallin possesses a globular pear-like shape, incompatible with the shape of the crystallographic domain-swapped dimer. The face-en-face dimer structure seemed to fit reasonably well into the globular shape, although the narrow end of the envelope did not appear to contain any structure. We reasoned that the protrusion may be associated with the disordered, flexible terminal extensions. This was confirmed by further SAXS analysis of the truncated βB2-crystallin, which does not contain

terminal extensions. Since the protrusion is not present in the SAXS envelope of the truncated βB2-crystallin, we can clearly state that the narrow end of the pear-shaped envelope arises from the extensions in full-length human βB2-crystallin. Contact information between the domains obtained via PRE measurements further corroborated that no domain-swapped dimer was present in solution, while the PREs were compatible with a face-en-face dimer structure.

General rules associated with domain-swapping of proteins observed in crystal structures are still elusive, although the identity of residues in the hinge-loop regions as well as their lengths were found to play a role in some domain-swapped proteins (Ding et al., 2006; Gronenborn, 2009; Rousseau et al., 2003). For the β-crystallins, however, neither the linker length nor its sequence appears to be unique or special in βB2-crystallin. The crystal structures of γB- and truncated βB1-crystallin, which possess identical linker lengths to βB2-crystallin, do not exhibit domain swapping, and changing of the six-residue linker peptide sequence in monomeric γB-crystallin to the βB2-crystallin sequence did not change its monomeric state (Ebersbach et al., 2007; Mayr et al., 1994; Van Montfort et al., 2003).

Interestingly, βB2-crystallin is thermodynamically the least stable human β-crystallin, and the low-stability has been proposed to be associated with dynamical subunit exchange between βB2 and other β-crystallins (Bateman et al., 2003; Macdonald et al., 2005), and its presence in a variety of β-crystallin complexes (Ajaz et al., 1997). However, no structures of βB2-crystallin complexes with other crystallins are available, leaving the question open, whether βB2-crystallin could undergo domain-swapping in solution and how it regulates the formation and stability of β-crystallin oligomers. It may well be the case that for human βB2-crystallin alone, a domain-swapped structure only exists in the crystal, brought about by high protein concentration and mildly destabilizing conditions.

In summary, our combined SAXS and NMR data revealed that human βB2-crystallin in solution does not exist as a domain-swapped dimer, but forms a face-en-face dimer, resembling half of the crystallographic tetramer and the dimer observed for the truncated human βB1-crystallin.

Experimental Procedures

Cloning, protein expression and purification

The coding sequences of wild-type and truncated (residue 14–194) human βB2-crystallin were cloned into pET21a expression vectors. The C37V mutant was constructed by site-directed mutagenesis using appropriate primers for the amino acid change. All proteins were expressed in *E. coli* BL21(DE3). In brief, cells were grown at 37 °C until an OD_{600} of 0.6 was reached, and protein expression was induced using 0.5 mM IPTG at 37 °C for an additional 4 h. For uniform ^{2}H, ^{15}N and ^{13}C labeling, cells were grown in modified minimal medium, containing $^{2}H_2O$, $^{15}NH_4Cl$ and ^{2}H, $^{13}C_6$-glucose as the sole deuterium, nitrogen and carbon sources, respectively. For amino acid selective unlabeling, the desired amino acid was added 1 h before IPTG induction to a final concentration of 1 g/L. Cells were harvested by centrifugation and resuspended in 25 mM sodium phosphate buffer, pH 6.5, 1 mM DTT, 1 mM EDTA, lysed by sonication, and the cell debris was removed by centrifugation at

100,000*g* for 1 h at 4 °C. The supernatant was collected and applied to a Mono S 10/100 GL cation exchange column (GE Healthcare), equilibrated with 25 mM sodium phosphate buffer, pH 6.5, 1 mM DTT, 1 mM EDTA. Bound proteins were eluted using a 0–1 M NaCl gradient over a 12-column volume. Protein fractions containing βB2-crystallin were further purified over a Superdex 75 26/60 column (GE Healthcare) in 25 mM sodium phosphate buffer, pH 6.5, 5 mM DTT, 1 mM EDTA.

Multi-angle static light scattering

Multi-angle light scattering (MALS) data were obtained using a Superdex 200 10/300 GL column (GE Healthcare) with in-line multi-angle light scattering (Dawn HELEOS, Wyatt Technology) and refractive index detectors (Optilab rEX, Wyatt Technology). Protein samples were loaded onto the pre-equilibrated column at room temperature and eluted with 25 mM sodium phosphate buffer, pH 6.5, 5 mM DTT, 1 mM EDTA at a flow-rate of 0.5 ml/min. The molecular masses were calculated using the ASTRA program (Wyatt Technology).

Small angle X-ray scattering measurements and analysis

Solutions of wild-type full-length and truncated βB2-crystallin were prepared in 25 mM sodium phosphate buffer (pH 6.5, 5 mM DTT, 1 mM EDTA) at different concentrations. All SAXS data were collected at beamline 12-ID-B of the Advanced Photon Source at Argonne National Laboratory (Lemont, IL, USA) using X-rays of energy 14 keV ($\lambda \approx 0.8856$ Å). For each measurement, 30 individual exposures of 1 sec each were collected, compared to check for radiation damage, and averaged to yield the final scattering curves. Buffer scattering measurements were performed in an equivalent fashion and subtracted from the protein scattering data. All data were processed and analyzed using tools from the ATSAS software package (Petoukhov et al., 2012) including PRIMUS, GNOM, DATPOROD, DAMMIF, DAMAVER, DAMMIN and CRYSOL. The molecular masses were determined separately using SAXS MoW2 (Fischer et al., 2010), based on the Porod volumes calculated with DATPOROD and excluded volumes obtained from *ab initio* dummy atom models calculated in DAMMIN. R_g values and $P(r)$ distribution functions were determined with GNOM and PRIMUS. Ten individual bead models were calculated in DAMMIF. The alignment and averaging were calculated with DAMAVER to generate the most probable model, which was further refined in DAMMIN to give the final SAXS envelope. The final envelope was superimposed onto the crystal structure of βB2-crystallin using the program Situs (Wriggers, 2012). Experimental SAXS data and derived models of both full-length and terminally truncated βB2-crystallin have been deposited into the Small Angle Scattering Biological Data Bank (SASBDB) (Valentini et al., 2015) with the accession codes SASDBT9 and SASDBU9.

Nitroxide spin labeling of the C37V mutant

Purified C37V βB2-crystallin at a concentration of 25 μM was used for labeling with (1-oxyl-2,2,5,5-tetramethyl-Δ3-pyrroline-3-methyl) methanethiosulfonate (MTSL) and the diamagnetic analog of MTSL, (1-acetyl-2,2,5,5-tetramethyl-Δ3-pyrroline-3-methyl) methanethiosulfonate (Toronto Research Chemicals Inc.) in parallel reactions by adding MTSL or dMTSL at 5-fold molar excess to protein, using 40 mM stock solutions. The reaction mixtures were incubated at 4 °C, and the excess, unreacted spin-labels were

removed by extensive dialysis against 25 mM sodium phosphate buffer, pH 6.5, 1 mM EDTA. Mixed samples were prepared by mixing the dMTSL-modified ^{15}N-C37V mutant with either MTSL-modified ^{14}N-C37V or dMTSL-modified ^{14}N-C37V proteins at equal molar ratios. The mixed samples were incubated at 4 °C for 20 h prior to PRE measurements.

NMR spectroscopy

All NMR data were recorded at 308 K on Bruker 700-, 800-, and 900-MHz Avance spectrometers, equipped with triple resonance, *z*-axis gradient cryoprobes. Spectra were processed with NMRPipe (Delaglio et al., 1995), and analyzed using CcpNmr (Vranken et al., 2005) and Sparky (http://www.cgl.ucsf.edu/home/sparky/). TROSY-based 2D ^{1}H-^{15}N HSQC and 3D HNCA, HNCACB, and HNCOCACB experiments were performed for backbone assignments of the fully deuterated ^{13}C,^{15}N-labeled βB2-crystallin. Non-uniform sampling (Hyberts et al., 2010) was used for 3D data collection to improve resolution. Approximately 33% of the total indirect grid of ^{15}N × ^{13}C increments was recorded. Points were selected according to Poisson gap sampling (Hyberts et al., 2010), and the spectra were reconstructed using istHMS software (Hyberts et al., 2012). To further confirm some of the assignments, 2D ^{1}H-^{15}N HSQC spectra of amino acid selectively unlabeled samples were collected. Eight amino acids were chosen for selective unlabeling: Ser, Thr, His, Arg, Phe, Tyr, Lys and Gln. In order to measure PRE effects, 2D ^{1}H-^{15}N HSQC spectra were recorded without relaxation delay on the MTSL-, or dMTSL-modified ^{15}N-labeled C37V mutant βB2-crystallin. For PRE measurements on the mixed samples, the experiments were carried out with different T_2 relaxation delays (1 ms, 2 ms, 4 ms, 8 ms, and 12 ms).

Supplementary Material

Refer to Web version on PubMed Central for supplementary material.

Acknowledgments

This work was funded by the National Institutes of Health (grant EY021193 to A.M.G.) and made use of the SAXS Core Facility of the Center for Cancer Research, National Cancer Institute. Time on the shared scattering beamline 12-ID-B was allocated under the PUP-24152 agreement between the National Cancer Institute and Argonne National Laboratory (ANL). The Advanced Photon Source, a U.S. Department of Energy (DOE) Office of Science User Facility, is operated by Argonne National Laboratory under Contract No. DE-AC02-06CH11357. Drs. In-Ja Byeon and Elena Matei are gratefully acknowledged for advice regarding NMR spectroscopy and Mike Delk for NMR technical support.

References

Ajaz MS, Ma Z, Smith DL, Smith JB. Size of human lens β-crystallin aggregates are distinguished by N-terminal truncation of βB1. J Biol Chem. 1997; 272:11250–11255. [PubMed: 9111027]

Andley UP. Crystallins in the eye: Function and pathology. Prog Retin Eye Res. 2007; 26:78–98. [PubMed: 17166758]

Bateman OA, Lubsen NH, Slingsby C. Association behaviour of human βB1-crystallin and its truncated forms. Exp Eye Res. 2001; 73:321–331. [PubMed: 11520107]

Bateman OA, Sarra R, van Genesen ST, Kappe G, Lubsen NH, Slingsby C. The stability of human acidic β-crystallin oligomers and hetero-oligomers. Exp Eye Res. 2003; 77:409–422. [PubMed: 12957141]

Bateman OA, Slingsby C. Structural studies on βH-crystallin from bovine eye lens. Exp Eye Res. 1992; 55:127–133. [PubMed: 1397121]

Bax B, Lapatto R, Nalini V, Driessen H, Lindley PF, Mahadevan D, Blundell TL, Slingsby C. X-Ray analysis of βB2-crystallin and evolution of oligomeric lens proteins. Nature. 1990; 347:776–780. [PubMed: 2234050]

Bewley CA, Gustafson KR, Boyd MR, Covell DG, Bax A, Clore GM, Gronenborn AM. Solution structure of cyanovirin-N, a potent HIV-inactivating protein. Nat Struct Mol Biol. 1998; 5:571–578.

Bloemendal H, de Jong W, Jaenicke R, Lubsen NH, Slingsby C, Tardieu A. Ageing and vision: structure, stability and function of lens crystallins. Prog Biophys Mol Biol. 2004; 86:407–485. [PubMed: 15302206]

Carver JA, Cooper PG, Truscott RJW. 1H-NMR spectroscopy of βB2-crystallin from bovine eye lens - conformation of the N- and C-terminal extensions. Eur J Biochem. 1993; 213:313–320. [PubMed: 8477703]

Clore GM, Gronenborn AM. Determination of three-dimensional structures of proteins and nucleic acids in solution by nuclear magnetic resonance spectroscopy. Crit Rev Biochem Mol Biol. 1989; 24:479–564. [PubMed: 2676353]

Clore GM, Gronenborn AM. Applications of three- and four-dimensional heteronuclear NMR-spectroscopy to protein-structure determination. Prog Nucl Magn Reson Spectrosc. 1991; 23:43–92.

Cooper PG, Carver JA, Truscott RJ. 1H-NMR spectroscopy of bovine lens β-crystallin - the role of the βB2-crystallin C-terminal extension in aggregation. Eur J Biochem. 1993; 213:321–328. [PubMed: 8477704]

Delaglio F, Grzesiek S, Vuister GW, Zhu G, Pfeifer J, Bax A. NMRPipe - a multidimensional spectral processing system based on UNIX pipes. J Biomol NMR. 1995; 6:277–293. [PubMed: 8520220]

Ding F, Prutzman KC, Campbell SL, Dokholyan NV. Topological determinants of protein domain swapping. Structure. 2006; 14:5–14. [PubMed: 16407060]

Ebersbach H, Fiedler E, Scheuermann T, Fiedler M, Stubbs MT, Reimann C, Proetzel G, Rudolph R, Fiedler U. Affilin-novel binding molecules based on human γ-B-crystallin, an all β-sheet protein. J Mol Biol. 2007; 372:172–185. [PubMed: 17628592]

Feng JH, Smith DL, Smith JB. Human lens β-crystallin solubility. J Biol Chem. 2000; 275:11585–11590. [PubMed: 10766773]

Fischer H, Neto MD, Napolitano HB, Polikarpov I, Craievich AF. Determination of the molecular weight of proteins in solution from a single small-angle X-ray scattering measurement on a relative scale. J Appl Crystallogr. 2010; 43:101–109.

Gronenborn AM. Protein acrobatics in pairs - dimerization via domain swapping. Curr Opin Struct Biol. 2009; 19:39–49. [PubMed: 19162470]

Haslbeck M, Peschek J, Buchner J, Weinkauf S. Structure and function of α-crystallins: traversing from in vitro to in vivo. Biochim Biophys Acta. 2016; 1860:149–166.

Hyberts SG, Milbradt AG, Wagner AB, Arthanari H, Wagner G. Application of iterative soft thresholding for fast reconstruction of NMR data non-uniformly sampled with multidimensional Poisson Gap scheduling. J Biomol NMR. 2012; 52:315–327. [PubMed: 22331404]

Hyberts SG, Takeuchi K, Wagner G. Poisson-Gap sampling and forward maximum entropy reconstruction for enhancing the resolution and sensitivity of protein NMR data. J Am Chem Soc. 2010; 132:2145–2147. [PubMed: 20121194]

Koharudin LMI, Liu L, Gronenborn AM. Different 3D domain-swapped oligomeric cyanovirin-N structures suggest trapped folding intermediates. Proc Natl Acad Sci USA. 2013; 110:7702–7707. [PubMed: 23610431]

Kroone RC, Elliott GS, Ferszt A, Slingsby C, Lubsen NH, Schoenmakers JGG. The role of the sequence extensions in β-crystallin assembly. Protein Eng. 1994; 7:1395–1399. [PubMed: 7700872]

Liu L, Byeon IJL, Bahar I, Gronenborn AM. Domain swapping proceeds via complete unfolding: a 19F- and 1H-NMR study of the cyanovirin-N Protein. J Am Chem Soc. 2012; 134:4229–4235. [PubMed: 22296296]

Liu Y, Eisenberg D. 3D domain swapping: As domains continue to swap. Protein Sci. 2002; 11:1285–1299. [PubMed: 12021428]

Macdonald JT, Purkiss AG, Smith MA, Evans P, Goodfellow JM, Slingsby C. Unfolding crystallins: The destabilizing role of a β-hairpin cysteine in βB2-crystallin by simulation and experiment. Protein Sci. 2005; 14:1282–1292. [PubMed: 15840832]

Marin-Vinader L, Onnekink C, van Genesen ST, Slingsby C, Lubsen NH. In vivo heteromer formation. Expression of soluble βA4-crystallin requires coexpression of a heteromeric partner FEBS J. 2006; 273:3172–3182.

Mayr EM, Jaenicke R, Glockshuber R. Domain interactions and connecting peptides in lens crystallins. J Mol Biol. 1994; 235:84–88. [PubMed: 8289268]

O'Connell MR, Gamsjaeger R, Mackay JP. The structural analysis of protein-protein interactions by NMR spectroscopy. Proteomics. 2009; 9:5224–5232. [PubMed: 19834907]

Overduin M, Harvey TS, Bagby S, Tong KI, Yau P, Takeichi M, Ikura M. Solution structure of the epithelial cadherin domain responsible for selective cell-adhesion. Science. 1995; 267:386–389. [PubMed: 7824937]

Petoukhov MV, Franke D, Shkumatov AV, Tria G, Kikhney AG, Gajda M, Gorba C, Mertens HDT, Konarev PV, Svergun DI. New developments in the ATSAS program package for small-angle scattering data analysis. J Appl Crystallogr. 2012; 45:342–350. [PubMed: 25484842]

Qin J, Vinogradova O, Gronenborn AM. Protein-protein interactions probed by nuclear magnetic resonance spectroscopy. Methods Enzymol. 2001; 339:377–389. [PubMed: 11462822]

Robinson NE, Lampi KJ, Speir JP, Kruppa G, Easterling M, Robinson AB. Quantitative measurement of young human eye lens crystallins by direct injection Fourier transform ion cyclotron resonance mass spectrometry. Mol Vis. 2006; 12:704–711. [PubMed: 16807530]

Rousseau F, Schymkowitz JWH, Itzhaki LS. The unfolding story of three-dimensional domain swapping. Structure. 2003; 11:243–251. [PubMed: 12623012]

Shapiro L, Fannon AM, Kwong PD, Thompson A, Lehmann MS, Grubel G, Legrand JF, Alsnielsen J, Colman DR, Hendrickson WA. Structural basis of cell-cell adhesion by cadherins. Nature. 1995; 374:327–337. [PubMed: 7885471]

Slingsby C, Wistow GJ. Functions of crystallins in and out of lens: roles in elongated and post-mitotic cells. Prog Biophys Mol Biol. 2014; 115:52–67. [PubMed: 24582830]

Smith MA, Bateman OA, Jaenicke R, Slingsby C. Mutation of interfaces in domain-swapped human βB2-crystallin. Protein Sci. 2007; 16:615–625. [PubMed: 17327390]

Takemoto L, Sorensen CM. Protein-protein interactions and lens transparency. Exp Eye Res. 2008; 87:496–501. [PubMed: 18835387]

Trinkl S, Glockshuber R, Jaenicke R. Dimerization of βB2-crystallin - the role of the linker peptide and the N- and C-terminal extensions. Protein Sci. 1994; 3:1392–1400. [PubMed: 7833801]

Valentini E, Kikhney AG, Previtali G, Jeffries CM, Svergun DI. SASBDB, a repository for biological small-angle scattering data. Nucleic Acids Res. 2015; 43:D357–D363. [PubMed: 25352555]

Van Montfort RLM, Bateman OA, Lubsen NH, Slingsby C. Crystal structure of truncated human βB1-crystallin. Protein Sci. 2003; 12:2606–2612. [PubMed: 14573871]

Vranken WF, Boucher W, Stevens TJ, Fogh RH, Pajon A, Llinas P, Ulrich EL, Markley JL, Ionides J, Laue ED. The CCPN data model for NMR spectroscopy: development of a software pipeline. Proteins. 2005; 59:687–696. [PubMed: 15815974]

Wriggers W. Conventions and workflows for using Situs. Acta Crystallogr D Biol Crystallogr. 2012; 68:344–351. [PubMed: 22505255]

Zhang Z, David LL, Smith DL, Smith JB. Resistance of human βB2-crystallin to in vivo modification. Exp Eye Res. 2001; 73:203–211. [PubMed: 11446770]

Zhang Z, Smith DL, Smith JB. Human β-crystallins modified by backbone cleavage, deamidation and oxidation are prone to associate. Exp Eye Res. 2003; 77:259–272. [PubMed: 12907158]

In Brief

Xi et al. combine MALS, SAXS and NMR to show that human βB2-crystallin forms a face-en-face dimer in solution, in contrast to the crystallographic domain-swapped dimer, demonstrating that protein quaternary structures can be significantly influenced by experimental conditions.

Highlights

- Full-length and terminally truncated βB2-crystallin form dimers in solution
- SAXS and NMR PRE data reveal a face-en-face dimer, not a domain-swapped structure
- The solution dimer resembles half of the lattice tetramer
- The dimeric arrangement is similar to the crystallographic dimer of truncated βB1

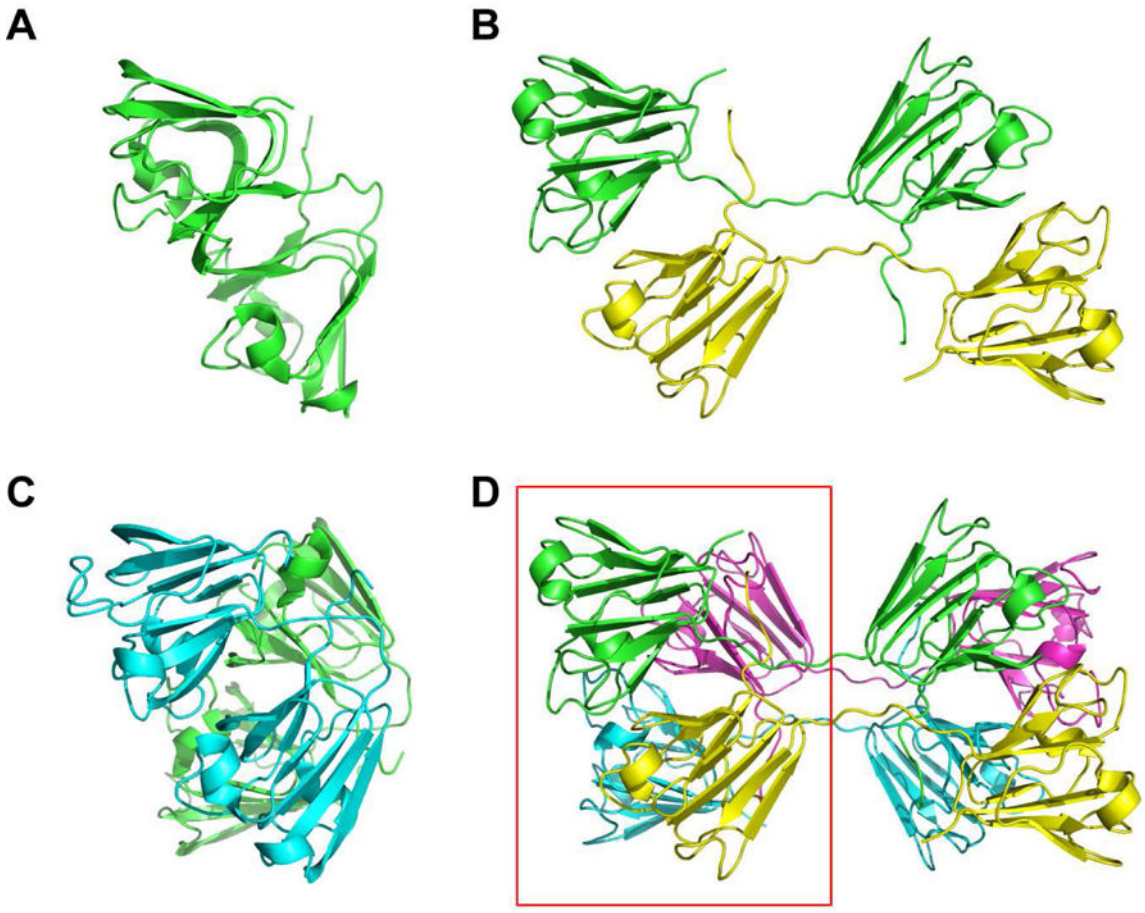

Figure 1.

Crystal structures of human βγ-crystallins. (**A**) Monomeric γD-crystallin (PDB code: 1HK0). (**B**) Domain-swapped dimer of βB2-crystallin (PDB code 1YTQ). (**C**) Dimeric truncated βB1-crystallin (PDB code 1OKI). (**D**) The lattice tetramer of βB2-crystallin. One half of the tetramer (boxed in red) resembles the crystal structure of dimeric truncated βB1-crystallin.

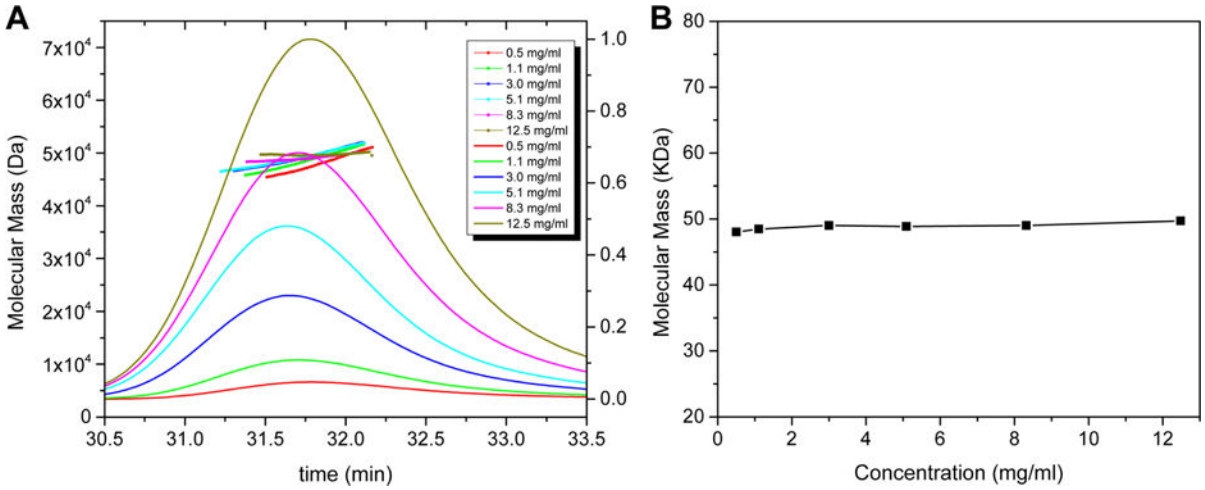

Figure 2.

Concentration dependence of the molecular mass of full-length βB2 crystallin using size-exclusion chromatography (Superdex200 10/300 GL) in conjunction with in-line multi-angle light scattering and refractive index detection. (**A**) Elution profiles with the predicted molecular masses shown by rectangles. (**B**) Plot of the estimated molecular masses as a function of protein concentration.

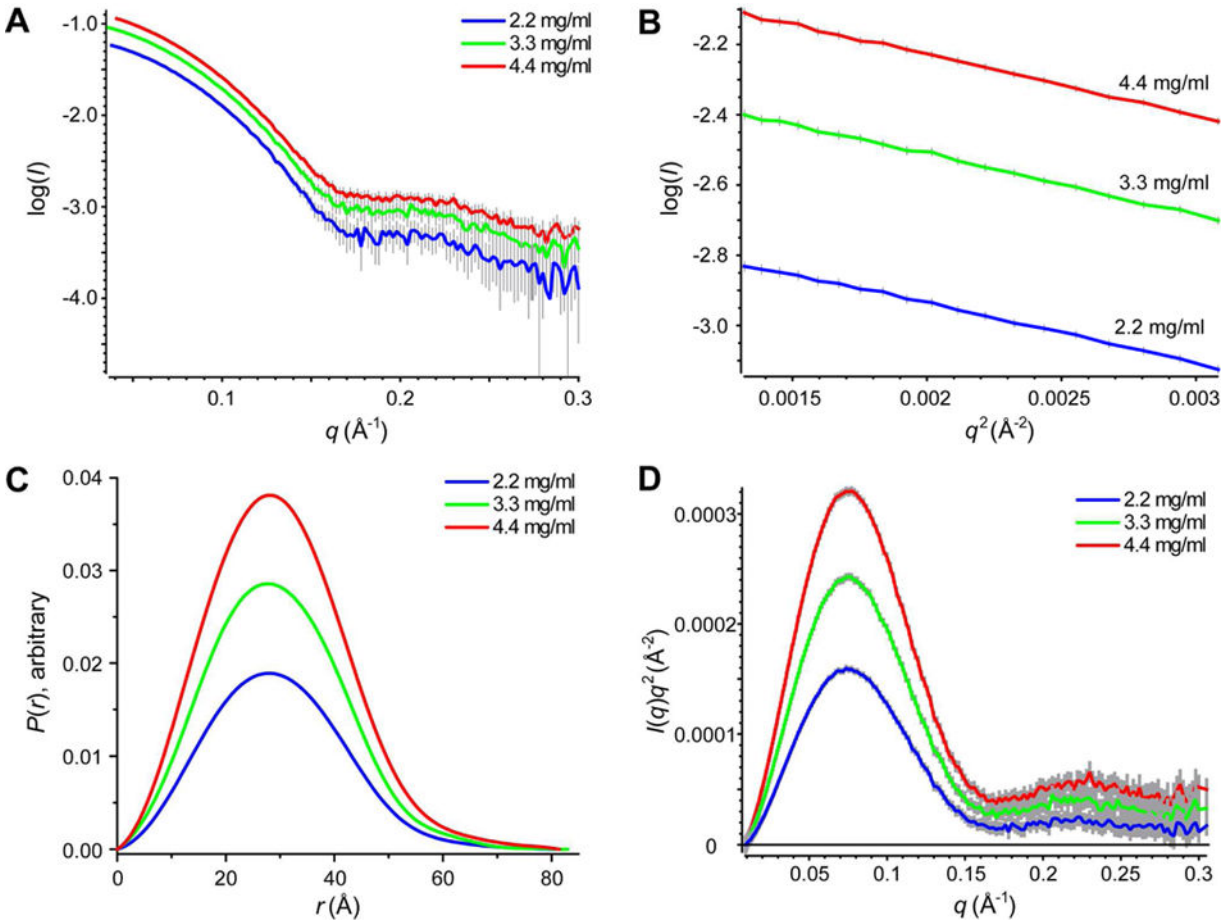

Figure 3.

SAXS analysis of full-length βB2-crystallin at different concentrations. (**A**) Background-subtracted SAXS intensity profiles and (**B**) Guinier plots for three different concentrations. (**C**) Pair-wise distance distribution function *P*(*r*) and (**D**) Kratky plots. See also Figure S1 and Table S1.

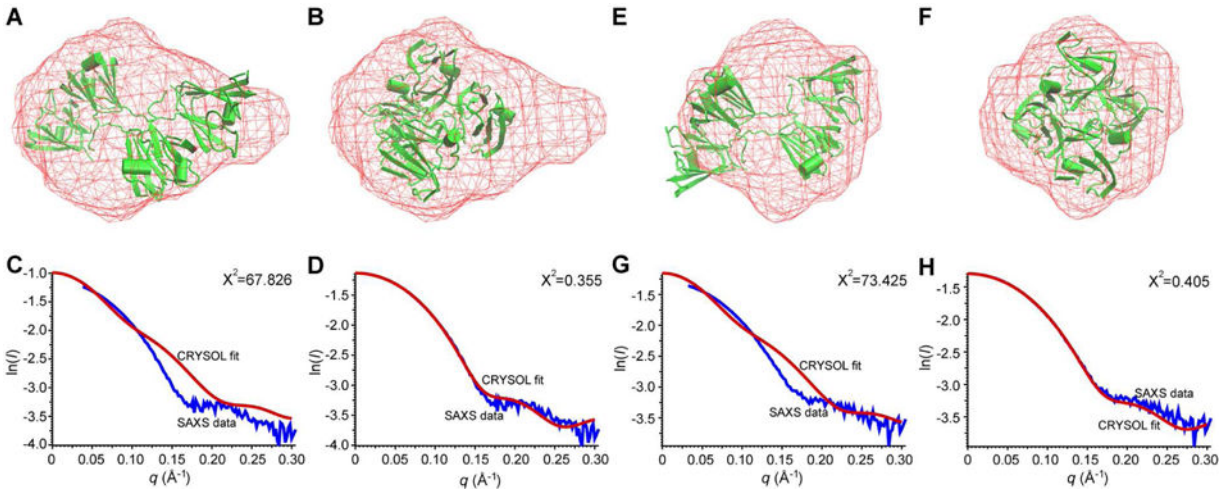

Figure 4.

SAXS-derived protein envelopes of full-length and truncated βB2-crystallin. The crystal structures of the domain-swapped dimer (**A**,**E**) and a pseudo face-en-face dimer (half of the lattice tetramer of βB2-crystallin, see boxed region in Figure 1D) (**B**,**F**) are embedded into the SAXS envelopes (red surface mesh) of full-length (**A**,**B**) and truncated (**E**,**F**) βB2-crystallin. Comparison of the theoretical scattering profiles calculated by CRYSOL (red traces), using the coordinates of the domain-swapped dimer (**C**,**G**) and the pseudo face-en-face dimer (**D**,**H**), with the experimental scattering data (blue traces) of full-length (**C**,**D**) and truncated βB2-crystallin (**G**,**H**). See also Figure S2, S3 and Table S2.

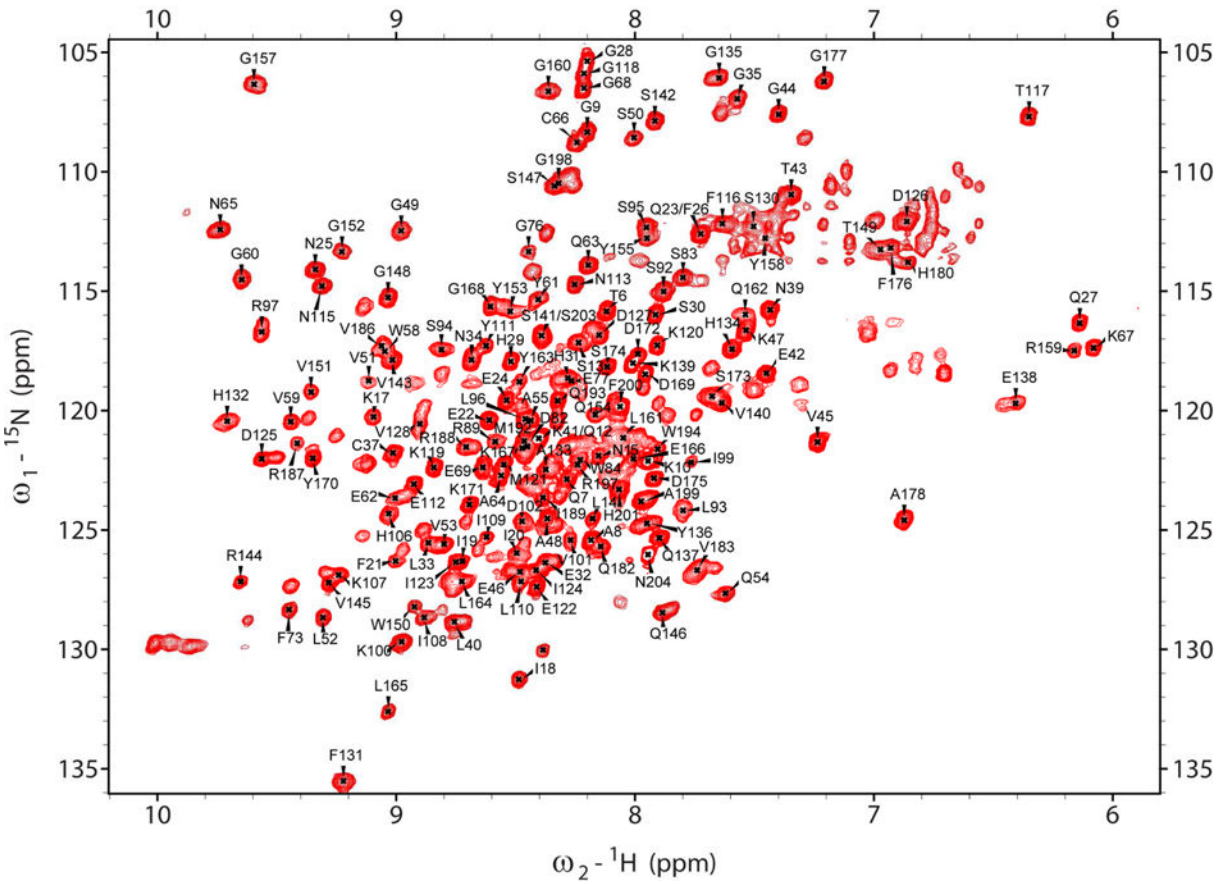

Figure 5.

800 MHz ^{1}H-^{15}N TROSY-HSQC spectrum of 350 μM triple ^{13}C,^{15}N,^{2}H-labeled full-length βB2-crystallin. Assignments are indicated by residue name and number.

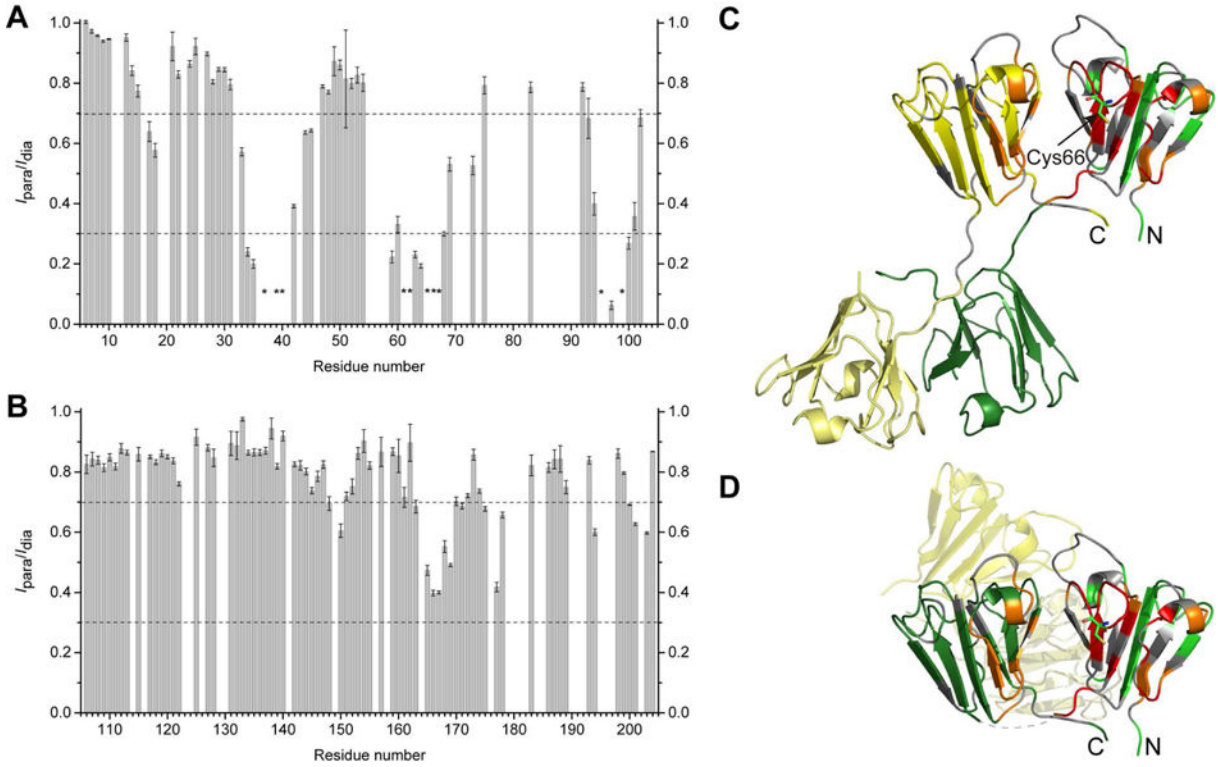

Figure 6.

^{1}H PRE data of the ^{15}N-labeled C37V mutant of full-length dimeric βB2-crystallin, containing a paramagnetic tag in the N-terminal domain. Signal intensity ratios for MTSL- and dMTSL-labeled protein are plotted as a function of residue number for the N-terminal domain in (**A**) and the C-terminal domain in (**B**). Data for overlapping or unassigned resonances are not included. Residues whose resonances were broadened beyond detection after MTSL-labeling are marked with asterisks. Structural mapping of the PRE effects onto the domain-swapped dimer (**C**) and the pseudo face-en-face dimer (half of the βB2-crystallin lattice tetramer, see boxed region in Figure 1D) (**D**). Residues that are associated with large PRE effects (I_{para}/I_{dia}<0.3) are colored red, those exhibiting medium and moderate PRE effects (0.3<I_{para}/I_{dia}<0.7) orange, and those with small or no effects (I_{para}/I_{dia}>0.7) unchanged. Residues with overlapping or unassigned resonances are colored gray. See also Figure S4.

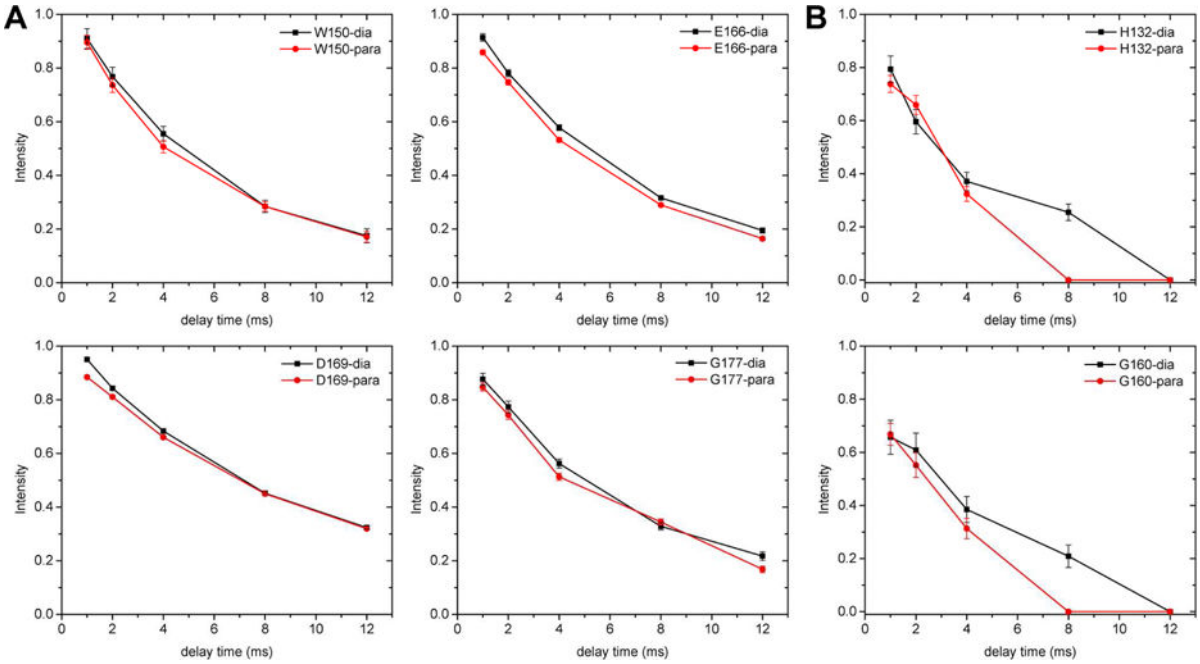

Figure 7.

Resonance intensity decays for several residues in the 1:1 mixed samples of full-length dMTSL-^{15}N-C37V:MTSL-^{14}N-C37V and dMTSL-^{15}N-C37V:dMTSL-^{14}N-C37V βB2-crystallin. The normalized resonance intensities of the paramagnetic (red) and diamagnetic (black) sample are plotted for different T_2 relaxation delays. (**A**) PRE effects are expected to be observable for a domain-swapped dimer, but not a face-en-face dimer. (**B**) PRE effects observed on the His132 and G160 amide resonances compatible with a face-en-face dimer. See also Figure S5 and S6.